

1 **Quantifying SO<sub>2</sub> oxidation pathways to atmospheric sulfate by using**  
2 **stable sulfur and oxygen isotopes: laboratory simulation and field**  
3 **observation**

4 Ziyang Guo<sup>a</sup>, Keding Lu<sup>a\*</sup>, Pengxiang Qiu<sup>b</sup>, Mingyi Xu<sup>b</sup>, Zhaobing Guo<sup>b\*</sup>

5  
6 <sup>a</sup> State Key Joint Laboratory of Environmental Simulation and Pollution Control,  
7 State Environmental Protection Key Laboratory of Atmospheric Ozone Pollution  
8 Control, College of Environmental Sciences and Engineering, Peking University,  
9 Beijing, China.

10 <sup>b</sup> Jiangsu Key Laboratory of Atmospheric Environment Monitoring and Pollution  
11 Control (AEMPC), Collaborative Innovation Center of Atmospheric Environment and  
12 Equipment Technology (CIC-AEET), School of Environmental Science and  
13 Engineering, Nanjing University of Information Science and Technology, Nanjing  
14 210044, China

15  
16 \* Correspondence to: [k.lu@pku.edu.cn](mailto:k.lu@pku.edu.cn) (Keding Lu), [guocumt@nuist.edu.cn](mailto:guocumt@nuist.edu.cn)  
17 (Zhaobing Guo)

19 **Abstract.** The formation of secondary sulfate in the atmosphere remains controversial, and it is urgent  
20 to seek for a new method to quantify different sulfate formation pathways. Thus, SO<sub>2</sub> and PM<sub>2.5</sub>  
21 samples were collected from 4 to 22 Dec. 2019 in Nanjing region. Sulfur and oxygen isotopic  
22 compositions were synchronously measured to study the contribution of SO<sub>2</sub> homogeneous and  
23 heterogeneous oxidation to sulfate. Meanwhile, the correlation of δ<sup>18</sup>O values between H<sub>2</sub>O and sulfate  
24 from SO<sub>2</sub> oxidation by H<sub>2</sub>O<sub>2</sub> and Fe<sup>3+</sup>/O<sub>2</sub> were simulatively investigated in the laboratory. Based on  
25 isotope mass equilibrium equations, the ratios of different SO<sub>2</sub> oxidation pathways were quantified. The  
26 results showed that secondary sulfate constituted higher than 80% of total sulfate in PM<sub>2.5</sub> during the  
27 sampling period. Laboratory simulation experiments indicated that δ<sup>18</sup>O value of sulfate was linearly  
28 dependent on δ<sup>18</sup>O value of water, and the slopes of linear curves for SO<sub>2</sub> oxidation by H<sub>2</sub>O<sub>2</sub> and  
29 Fe<sup>3+</sup>/O<sub>2</sub> were 0.43 and 0.65, respectively. The secondary sulfate in PM<sub>2.5</sub> was mainly ascribed to SO<sub>2</sub>  
30 homogeneous oxidation by OH radicals and heterogeneous oxidation by H<sub>2</sub>O<sub>2</sub> and Fe<sup>3+</sup>/O<sub>2</sub>. SO<sub>2</sub>  
31 heterogeneous oxidation was generally dominant during sulfate formation, and SO<sub>2</sub> oxidation by H<sub>2</sub>O<sub>2</sub>  
32 predominated in SO<sub>2</sub> heterogeneous oxidation reactions with an average ratio around 54.6%. This study  
33 provided an insight into precisely evaluating sulfate formation by combining stable sulfur and oxygen  
34 isotopes.

35  
36  
37  
38  
39  
40

## 41 **1 Introduction**

42 Sulfate is one of the prevalent components of PM<sub>2.5</sub> (Briggemann et al., 2021; Huang et al., 2014;  
43 Yang et al., 2023). Sulfate makes up approximately 25% of PM<sub>2.5</sub> mass in Shanghai, 23% in  
44 Guangzhou and 10-33% in Beijing (Xue et al., 2016). The rapid sulfate formation is a crucial factor  
45 determining the explosive growth of fine particles and the frequent occurrence of severe haze events in  
46 China (Lin et al., 2022; Liu et al., 2020; Meng et al., 2023; Wang et al., 2021). Sulfate plays an  
47 important role in the chemical and physical processes in the troposphere and lower stratosphere, which  
48 significantly affects global climate change by scattering solar radiation and acting as cloud  
49 condensation nuclei (Gao et al., 2022; Ramanathan et al., 2001). Meanwhile, sulfate exerts a significant  
50 influence on air quality and public health (Abbatt et al., 2006).

51 In the past decades, numerous attempts have been made to evaluate SO<sub>2</sub> oxidation pathways  
52 involving in homogeneous and heterogeneous reactions. Traditionally, sulfate formation mechanisms  
53 mainly include SO<sub>2</sub> homogeneous oxidation by OH radicals and heterogeneous oxidation by H<sub>2</sub>O<sub>2</sub>, O<sub>3</sub>  
54 and O<sub>2</sub> catalyzed by transition metal ions (TMIs) in cloud/fog water droplets. The relative importance  
55 of different sulfate formation pathways is strongly dependent on oxidant concentrations, occurrence of  
56 fog/cloud events and pH of aqueous phase (Kuang et al., 2022; Oh et al., 2023). Generally, SO<sub>2</sub>  
57 homogeneous oxidation by OH radicals and heterogeneous oxidation by H<sub>2</sub>O<sub>2</sub> are considered the most  
58 important pathways for sulfate production on the global scale (Seinfeld and Pandis, 1998). The  
59 photochemical reactivity during the winter in Beijing has been found to be relatively high, which  
60 favored the formation of reactive species such as OH radicals and H<sub>2</sub>O<sub>2</sub>, thereby facilitating SO<sub>2</sub>  
61 oxidation (Zhang et al., 2020). Xue et al. (2014) suggested that SO<sub>2</sub> oxidation by O<sub>3</sub> and H<sub>2</sub>O<sub>2</sub> in  
62 aqueous phase contributed to the majority of total sulfate production. Liu et al. (2020) proposed that  
63 S(IV) oxidation by H<sub>2</sub>O<sub>2</sub> in aerosol water could be an important pathway considering the ionic strength  
64 effect. He et al. (2018) found that the contribution of SO<sub>2</sub> oxidation by H<sub>2</sub>O<sub>2</sub> could reach 88% during  
65 Beijing haze period. Ye et al. (2018) observed that SO<sub>2</sub> oxidation rate by H<sub>2</sub>O<sub>2</sub> was 2-5 times faster  
66 than the summed rate of the other three oxidation pathways. As a result, actual contribution of SO<sub>2</sub>  
67 oxidation by H<sub>2</sub>O<sub>2</sub> during the winter might be underestimated in the previous studies.

68 In addition, the presence of NO<sub>2</sub> was obviously favorable for SO<sub>2</sub> oxidation under the conditions of  
69 high [relative humidity \(RH\)](#) and NH<sub>3</sub>. NH<sub>3</sub> can promote the hydrolysis of NO<sub>2</sub> dimers to HONO and

70 result in more sulfate formation on particle surface in humid conditions. However, this conclusion was  
71 doubted by Liu et al. (2017) who believed that the reaction on actual fine particles with pH at 4.2 was  
72 too slow to account for sulfate formation. Li et al. (2020) deemed that SO<sub>2</sub> oxidation by NO<sub>2</sub> might not  
73 be a major oxidation pathway in China. Furthermore, GEOS-Chem modeling study suggested that NO<sub>2</sub>  
74 oxidation contributed less than 2% of total sulfate production. It is found that TMI pathway was very  
75 important in highly polluted regions, and the contribution of metal-catalyzed SO<sub>2</sub> oxidation to sulfate  
76 was as high as 49±10% in haze. Wang et al. (2021) also argued that SO<sub>2</sub> oxidation via TMI on aerosol  
77 surface could be the dominant sulfate formation pathway. They found that manganese-catalyzed  
78 oxidation of SO<sub>2</sub> contributed 69.2±5.0% in sulfate production. Overall, the mechanisms for sulfate  
79 rapid growth remain unclear and controversial. Therefore, sulfate formation pathways need to be  
80 further explored, and it is urgent to develop a new method to quantify different sulfate formation  
81 processes.

82 Generally, sulfur isotopes allow for investigating SO<sub>2</sub> oxidation processes in the atmosphere because  
83 of distinctive isotope fractionation associated with different oxidation reactions (Harris et al., 2013).  
84 Harris et al. (2012) presented [the respective](#) sulfur isotope fractionation factors of SO<sub>2</sub> oxidation by OH,  
85 O<sub>3</sub>/H<sub>2</sub>O<sub>2</sub> and iron catalysis ~~were 1.0087, 1.0167 and 0.9905, respectively.~~ Besides, the observed sulfur  
86 isotope fractionation of SO<sub>2</sub> oxidation by H<sub>2</sub>O<sub>2</sub> and O<sub>3</sub> appeared to be no significant difference.  
87 Therefore, the results were particularly useful to determine the importance of transition metal-catalyzed  
88 oxidation pathway compared to other oxidation pathways. However, other main SO<sub>2</sub> oxidation  
89 pathways could not be distinguished only based on stable sulfur isotope determination.

90 Oxygen isotope ratio (δ<sup>18</sup>O) can be used to deduce sulfate formation processes due to those SO<sub>2</sub>  
91 oxidation pathways affect oxygen isotope of product sulfate differently. Especially, mass-independent  
92 fractionation signals of oxygen isotopes (nonzero Δ<sup>17</sup>O, where Δ<sup>17</sup>O=δ<sup>18</sup>O-0.52×δ<sup>17</sup>O) in sulfate are  
93 usually adopted to investigate the contribution of different SO<sub>2</sub> oxidation pathways. This method can  
94 identify the contribution of SO<sub>2</sub>+O<sub>3</sub> pathway when high Δ<sup>17</sup>O value (>3‰) is measured in sulfate.  
95 However, there is presence of obvious uncertainty when interpreting the sulfate with low Δ<sup>17</sup>O value  
96 (<1‰). Unfortunately, most sulfate samples in the atmosphere present Δ<sup>17</sup>O<1‰, suggesting a limited  
97 contribution of SO<sub>2</sub>+O<sub>3</sub> pathway during sulfate formation. It is noteworthy that the contribution of  
98 SO<sub>2</sub>+H<sub>2</sub>O<sub>2</sub> and TMI pathway is unclear if solely using Δ<sup>17</sup>O (Li et al., 2020). Holt and Kumar (1984)

带格式的: 字体: (默认) Times New Roman, 10 磅, 字体颜色: 自动设置, 图案: 清除

带格式的: 字体颜色: 自动设置

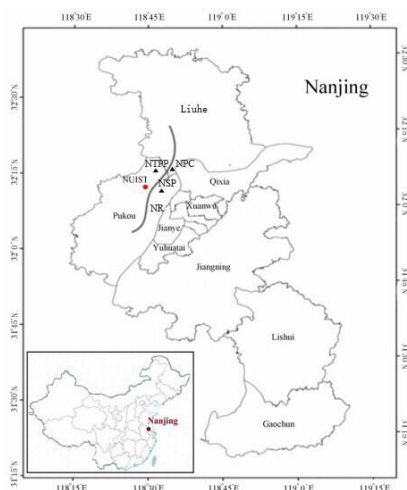
99 found oxygen isotope was a valuable and complementary method to determine probable mechanisms of  
100 SO<sub>2</sub> oxidation to sulfate in the atmosphere. This provides us an insight into precisely evaluating sulfate  
101 formation pathways by combining oxygen and sulfur isotopes.

102 In this contribution, PM<sub>2.5</sub> and SO<sub>2</sub> were sampled from 4 to 22 Dec. 2019 in Nanjing. Sulfur and  
103 oxygen isotopic compositions were measured to study the contribution of SO<sub>2</sub> homogeneous and  
104 heterogeneous oxidation during sulfate formation. In addition, the linear relationships of δ<sup>18</sup>O values  
105 between H<sub>2</sub>O and sulfate from SO<sub>2</sub> oxidation by H<sub>2</sub>O<sub>2</sub> and Fe<sup>3+</sup>/O<sub>2</sub> were synchronously investigated in  
106 the laboratory. Based on sulfur and oxygen isotopes mass equilibrium equations, the ratios of different  
107 SO<sub>2</sub> oxidation pathways during the sampling period were calculated. The study aims to seek for a novel  
108 method to quantify different SO<sub>2</sub> oxidation processes with sulfur and oxygen isotopes.

## 109 2 Materials and methods

### 110 2.1 Sampling location

111 PM<sub>2.5</sub> and SO<sub>2</sub> in the atmosphere were sampled from 4 to 22 Dec. 2019 in Nanjing, China. The  
112 sampling site was located at the roof of the library in Nanjing University of Information Science &  
113 Technology (NUIST, 32.1 °N, 118.5 °E), which is depicted in Fig. 1. The sampling location is at the  
114 side of Ningliu Road and closely next to Nanjing chemical industry park. There is presence of some  
115 large-scale chemical enterprises such as Nanjing steel plant, Nanjing thermal power plants and Nanjing  
116 petrochemical company, which inevitably release lots of SO<sub>2</sub> and iron metal into the atmosphere.



117  
118 Fig. 1. Sampling site of NUIST in Nanjing, China. NSP: Nanjing steel plants; NTPP: Nanjing

119 thermal power plants; NPC: Nanjing petrochemical company; NR: Ningliu Road.

## 120 2.2 PM<sub>2.5</sub> and SO<sub>2</sub> Samples collection

121 PM<sub>2.5</sub> and SO<sub>2</sub> were sampled by using a modified JCH-1000 sampler (Juchuang Co., Qingdao) with  
122 a flow rate of 1.05 m<sup>3</sup> min<sup>-1</sup> from 8 am to 8 pm from 4 to 22 Dec. 2019. PM<sub>2.5</sub> and SO<sub>2</sub> were collected  
123 with quartz filter (203×254 mm, Munktell, Sweden) and glass fiber filter (203×254 mm, Tisch  
124 Environment INC, USA), respectively. The filters were incinerated in a muffle furnace at 450 °C for 2h  
125 and then preserved in the desiccators at room temperature. The glass fiber filters were firstly soaked in  
126 2% K<sub>2</sub>CO<sub>3</sub> and 2% glycerol solution for 2h and dried in DGG-9070A electric oven. SO<sub>2</sub> can be  
127 changed into sulfite immediately during the sampling.

## 128 2.3 Extractions of water-soluble sulfate

129 PM<sub>2.5</sub> sample filters were shredded and soaked in 400 mL of Milli-Q (18 MΩ) water for extractions  
130 of water-soluble sulfate. Filters were then isolated from solutions by centrifugation and sulfate was  
131 precipitated as BaSO<sub>4</sub> by adding 1 mol L<sup>-1</sup> BaCl<sub>2</sub>. After the filtration with 0.22 μm acetate membrane,  
132 BaSO<sub>4</sub> precipitate was rinsed with Milli-Q water to remove Cl<sup>-</sup>. Finally, BaSO<sub>4</sub> powders were calcined  
133 at 800 °C for 2h to obtain high purity BaSO<sub>4</sub>. In addition, a small amount of H<sub>2</sub>O<sub>2</sub> solution was added  
134 to oxidize sulfite to sulfate.

## 135 2.4 Laboratory simulation of SO<sub>2</sub> oxidation by H<sub>2</sub>O<sub>2</sub> and Fe<sup>3+</sup>/O<sub>2</sub>

136 For SO<sub>2</sub> oxidation by H<sub>2</sub>O<sub>2</sub>, 30 mL min<sup>-1</sup> Ar was firstly introduced into three kinds of different water  
137 about 30 min to drive out air. Sulfate was produced by adding 10 mL H<sub>2</sub>O<sub>2</sub> dilute solution (0.1 mL 30%  
138 H<sub>2</sub>O<sub>2</sub> in 50 mL water) to SO<sub>2</sub> in the reaction chamber at 10 °C. H<sub>2</sub>O<sub>2</sub> solution was agitated vigorously  
139 for 1min before admission of air. For SO<sub>2</sub> oxidation by Fe<sup>3+</sup>/O<sub>2</sub>, 2 mL min<sup>-1</sup> SO<sub>2</sub> and 2 mL min<sup>-1</sup> O<sub>2</sub>  
140 were simultaneously put into Fe<sup>3+</sup> dilute solution at 10 °C. Then, 10 mL 1 mL min<sup>-1</sup> BaCl<sub>2</sub> was added to  
141 prepare BaSO<sub>4</sub>. Oxygen isotopic compositions of product sulfate and three kinds of water were  
142 measured to study their linear relationships.

## 143 2.5 Sulfur and oxygen isotope determination

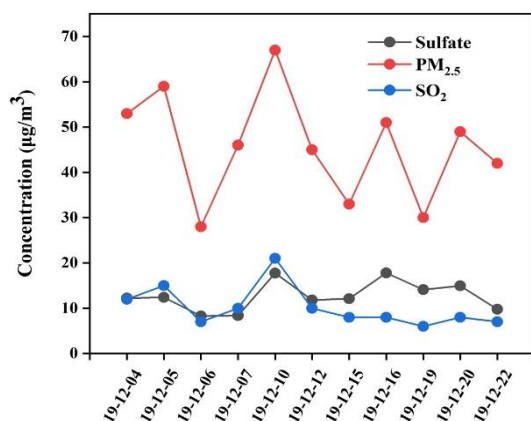
144 Sulfur isotopic compositions in sulfate were analyzed using Elemental analyzer (EA, Flash 2000,  
145 Thermo) and isotope mass spectrometer (IRMS, Delta V Plus, Finningan). High-purity BaSO<sub>4</sub> was  
146 converted into SO<sub>2</sub> in EA in the presence of Cu<sub>2</sub>O. SO<sub>2</sub> from EA was ionized and δ<sup>34</sup>S value was

147 measured using IRMS. For the determination of  $\delta^{18}\text{O}$ ,  $\text{BaSO}_4$  pyrolysis was conducted in graphite  
148 furnace at 1450 °C, and  $\delta^{18}\text{O}$  value was obtained in CO produced from the pyrolysis at continuous-flow  
149 mode. The results of  $\delta^{34}\text{S}$  and  $\delta^{18}\text{O}$  were with respect to international standard V-CDT and V-SMOW,  
150 and the accuracy were better than  $\pm 0.2\%$  and  $\pm 0.3\%$ , respectively.

### 151 3 Results and discussion

#### 152 3.1 Concentrations of $\text{PM}_{2.5}$ , sulfate and $\text{SO}_2$

153 As described in Fig. 2, the mass concentrations of  $\text{PM}_{2.5}$ ,  $\text{SO}_4^{2-}$  and  $\text{SO}_2$  during the period from 4 to  
154 22 Dec. 2019 in NUIST changed from 28.1 to 67.0  $\mu\text{g m}^{-3}$ , 8.3 to 17.8  $\mu\text{g m}^{-3}$  and 6.2 to 20.9  $\mu\text{g m}^{-3}$   
155 with an average and standard deviation at  $45.7\pm 12.1 \mu\text{g m}^{-3}$ ,  $12.7\pm 3.3 \mu\text{g m}^{-3}$  and  $10.2\pm 4.4 \mu\text{g m}^{-3}$ ,  
156 respectively. It can be observed that  $\text{PM}_{2.5}$  average concentration was about 1.3 times of the First Grade  
157 National Ambient Air Quality Standard ( $35 \mu\text{g m}^{-3}$ ) and beyond the safety standard of World Health  
158 Organization ( $10 \mu\text{g m}^{-3}$ ). The photochemical reactivity during the winter in Beijing has been found to  
159 be relatively high (Zhang et al., 2020), which facilitates the formation of some photooxidants. The  
160 relatively clean days during the sampling period indicates the importance of photoinduced oxidation of  
161  $\text{SO}_2$ .



162  
163 **Fig. 2. Variations in concentrations of  $\text{PM}_{2.5}$ ,  $\text{SO}_4^{2-}$  and  $\text{SO}_2$ .**

164 Meanwhile, the change trends of  $\text{PM}_{2.5}$ ,  $\text{SO}_4^{2-}$  and  $\text{SO}_2$  concentrations were found to be basically the  
165 same during the sampling period, indicating sulfate was mainly from  $\text{SO}_2$  oxidation. Especially,  $\text{PM}_{2.5}$ ,  
166  $\text{SO}_4^{2-}$  and  $\text{SO}_2$  concentrations increased to the maximum values on 10 Dec.. It is noted that  $\text{NO}_2$  and

带格式的: 下标

带格式的: 下标

带格式的: 上标

带格式的: 下标

167 CO concentrations were 85 and 1.60  $\mu\text{g m}^{-3}$  on 10 Dec., which were also the maximum values during  
168 the sampling period. Based on the wind speed was lower than  $3\text{m s}^{-1}$ , and there was presence of static  
169 weather during the sampling period, we believed that high CO concentration was mainly from local  
170 emissions. However,  $\text{O}_3$  concentration on 10 Dec. was the minimum value at  $24 \mu\text{g m}^{-3}$ , which  
171 preliminarily indicated that  $\text{SO}_2$  oxidation by  $\text{NO}_2$  might be a major pathway in sulfate formation.  
172 Previous studies showed that  $\text{SO}_2$  oxidation by  $\text{NO}_2$  in aerosol water dominated heterogeneous sulfate  
173 formation during wintertime at neutral aerosol pH (Wang et al., 2016; Cheng et al., 2016). However,  
174 subsequent studies showed that the calculated aerosol pH was in the range of 4.2~4.7, and the  
175 reactions between  $\text{SO}_2$  and  $\text{NO}_2$  during this pH range were too slow to produce sulfate. Taking into  
176 account low aerosol pH in Nanjing region, we suggested that  $\text{SO}_2$  oxidation by  $\text{NO}_2$  was not a  
177 dominant pathway for sulfate formation during the sampling period.

178 In contrast,  $\text{PM}_{2.5}$ ,  $\text{SO}_4^{2-}$  and  $\text{SO}_2$  concentrations were observed to be at the minimum values on 6  
179 Dec.. Similarly,  $\text{NO}_2$  and CO concentrations were also at the minimum of 36 and  $0.6 \text{mg m}^{-3}$ ,  
180 respectively. However,  $\text{O}_3$  concentration on 6 Dec. was the maximum at  $50 \mu\text{g m}^{-3}$ . Besides, the rate of  
181  $\text{SO}_2$  oxidation with  $\text{O}_3$  becomes fast only when  $\text{pH}>5$ , the reaction rate of  $\text{SO}_2$  with  $\text{O}_3$  is one hundredth  
182 of those with  $\text{H}_2\text{O}_2$  or TMI when  $\text{pH}<5$ . Therefore, pH values of actual fine particles at 4~5 in Nanjing  
183 region could markedly restrain  $\text{SO}_2$  oxidation by  $\text{O}_3$ . The lowest  $\text{SO}_4^{2-}$  concentration on 6 Dec. further  
184 demonstrated that  $\text{SO}_2$  oxidation by  $\text{O}_3$  played an insignificant role in sulfate formation.

185 Generally, aqueous-phase oxidation is deemed to be a main process of sulfate formation in  
186 atmospheric environment. Shao et al. (2018) believed that heterogeneous sulfate production on aerosols  
187 occurred when ~~relative humidity (RH)~~ was higher than 50 %. The RH values of the atmosphere ranging  
188 from 50.7 to 88.9% during the sampling period indicated that sulfate formation was closely related to  
189  $\text{SO}_2$  heterogeneous oxidation.

### 190 3.2 Sulfur isotopic compositions in sulfate and $\text{SO}_2$

191 It can be observed from Fig. 3 that the values of  $\delta^{34}\text{S-SO}_4^{2-}$  were generally higher compared to those  
192 of  $\delta^{34}\text{S-SO}_2$  during the sampling period except that on 16 Dec.. The  $\delta^{34}\text{S-SO}_4^{2-}$  values ranged from 3.1  
193 to 4.7‰ with an average and standard deviation at  $4.0\pm 0.6\%$ , while  $\delta^{34}\text{S-SO}_2$  values changed from -2.9  
194 to 4.7‰ with an average and standard deviation at  $-0.2\pm 2.3\%$ . The discrepancy between the values of  
195  $\delta^{34}\text{S-SO}_4^{2-}$  and  $\delta^{34}\text{S-SO}_2$  was mainly related to sulfur isotope fractionation effect during  $\text{SO}_2$  oxidation

带格式的: 字体: (中文) 宋体, 10 磅

带格式的: 字体: (中文) 宋体, 10 磅

带格式的: 字体: (中文) 宋体, 10 磅

带格式的: 上标

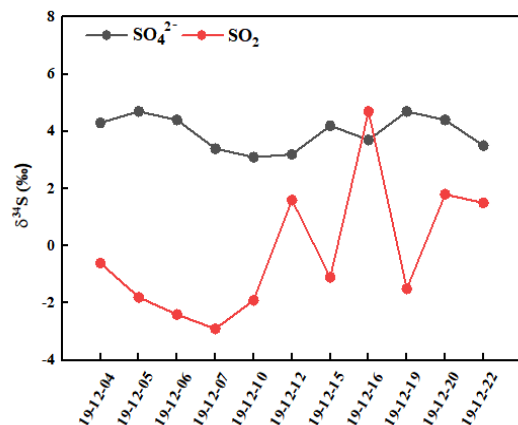
带格式的: 字体: (中文) 宋体, 10 磅

带格式的: 字体: (中文) 宋体, 10 磅

带格式的: 字体颜色: 红色



196 to secondary sulfate.

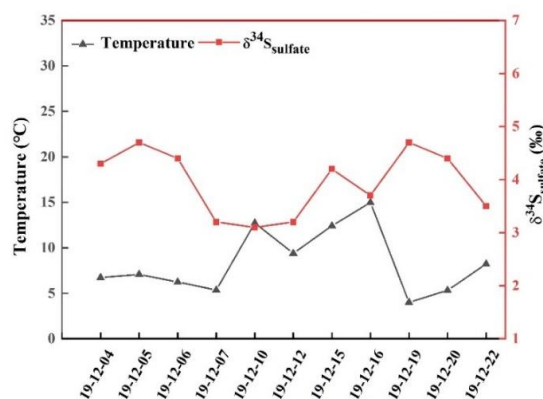


197  
198 **Fig. 3. Variations in sulfur isotopic compositions in sulfate and SO<sub>2</sub>**

带格式的: 下标

199 It is noteworthy that  $\delta^{34}\text{S-SO}_4^{2-}$  values were similar to that in  $\text{PM}_{2.5}$  with an average at 4.2‰ during  
200 Youth Olympic Games in Aug. 2014 in Nanjing (Guo et al., 2016). However, the average value of  
201  $\delta^{34}\text{S-SO}_4^{2-}$  during the sampling period was lower than 5.6‰ in Nanjing during a typical haze event  
202 from 21 Dec. 2015 to 1 Jan. 2016 (Guo et al., 2019). The higher  $\delta^{34}\text{S}$  values of sulfate in haze was  
203 possibly ascribed to  $\text{SO}_2$  heterogeneous oxidation, which typically enriched heavy sulfur isotope in  
204 sulfate. In this study, the average concentrations of  $\text{PM}_{2.5}$  was  $45.7 \mu\text{g m}^{-3}$ , indicating a not heavily  
205 polluted time interval. Besides, the relatively high temperature during the sampling period was  
206 favorable for photochemical reactions and OH radicals' formation. As a result, the contribution of  $\text{SO}_2$   
207 homogenous oxidation increased during sulfate formation, which enriched light sulfur isotope  
208 compared to that in haze. Han et al. (2017) determined  $\delta^{34}\text{S}$  values in Beijing  $\text{PM}_{2.5}$  with an average at  
209 6.0‰. It is observed that there existed a regional difference in  $\delta^{34}\text{S-SO}_4^{2-}$  values. The  $\delta^{34}\text{S-SO}_4^{2-}$  value  
210 in Nanjing was generally lower than that in Beijing. The discrepancy of  $\delta^{34}\text{S-SO}_4^{2-}$  value illustrated  
211 different sulfur sources and  $\text{SO}_2$  oxidation pathways in these regions. In addition,  $\delta^{34}\text{S-SO}_4^{2-}$  values  
212 presented a seasonal change.  $\delta^{34}\text{S}$  values in Beijing aerosol sulfate varied from 3.4 to 7.0‰ with a  
213 average of 5.0‰ in summer and from 7.1 to 11.3‰ with an average of 8.6‰ in winter. Generally,  $\text{SO}_2$   
214 homogeneous oxidation dominated in summer compared to that in winter due to strong solar irradiation  
215 (Han et al., 2016).  $\text{SO}_2$  oxidation might lead to sulfur isotope fractionation, which was mainly  
216 attributed to equilibrium or kinetic discrimination between  $\text{SO}_2$  and sulfate. The influence of different  
217 oxidants on sulfur isotope fractionation needed to be further investigated.

218 Fig.4 presents the relationship between  $\delta^{34}\text{S}\text{-SO}_4^{2-}$  value and atmospheric temperature during the  
 219 sampling period. It can be observed that there existed an obviously negative correlation. The higher  
 220 temperature generally corresponded to the lower  $\delta^{34}\text{S}\text{-SO}_4^{2-}$  value. This is mainly ascribed to kinetic  
 221 effect of sulfur isotope fractionation during  $\text{SO}_2$  oxidation. At high temperature, more OH radicals were  
 222 produced and the contribution of  $\text{SO}_2$  homogeneous oxidation increased. It is reported that sulfur  
 223 isotope fractionation about  $\text{SO}_2$  was -9‰ for homogeneous oxidation process (Tanaka et al., 1994).  
 224 Therefore, low  $\delta^{34}\text{S}$  value in sulfate at high temperature was chiefly due to elevated  $\text{SO}_2$  homogeneous  
 225 oxidation.



226  
 227 **Fig. 4.** The correlation between  $\delta^{34}\text{S}\text{-SO}_4^{2-}$  value and atmospheric temperature.

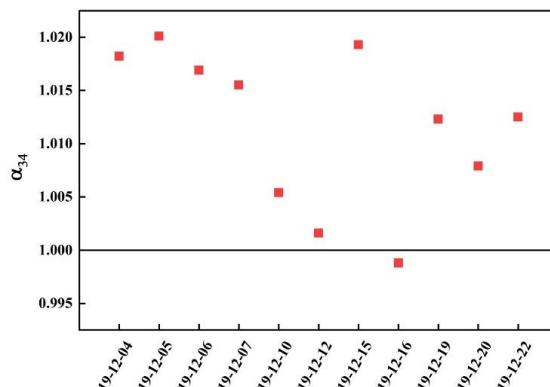
### 228 3.3 Sulfur isotope fractionation during $\text{SO}_2$ oxidation

229 The secondary sulfate was generally from  $\text{SO}_2$  homogeneous and heterogeneous oxidation (Seinfeld  
 230 and Pandis, 1998). The homogeneous and heterogeneous oxidation of  $\text{SO}_2$  might lead to sulfur isotope  
 231 fractionation, which is described by using fractionation coefficient ( $\alpha$ )

$$232 \alpha = \frac{\frac{\delta^{34}\text{S}_{\text{SO}_4^{2-}}}{10^3} + 1}{\frac{\delta^{34}\text{S}_{\text{SO}_2} + 1}{10^3}} \quad (1)$$

233 Sulfate enriched heavy sulfur isotope ( $\alpha > 1$ ) during  $\text{SO}_2$  heterogeneous oxidation for the presence of  
 234 isotope equilibrium fractionation and kinetic fractionation. However, sulfate enriched light sulfur  
 235 isotope ( $\alpha < 1$ ) during  $\text{SO}_2$  homogeneous oxidation due to this process was only related to kinetic  
 236 fractionation. As described in Fig. 5,  $\alpha$  values ranged from 0.9988 to 1.0201 indicating there existed  
 237  $\text{SO}_2$  homogeneous and heterogeneous oxidation during the sampling period.  $\alpha$  value was at the

238 minimum of 0.9988 on 16 Dec., which showed SO<sub>2</sub> homogeneous oxidation played a crucial role.



239

240 **Fig. 5.** Sulfur isotope fractionation coefficients during SO<sub>2</sub> oxidation.

241 It is reported that sulfur isotope fractionations during SO<sub>2</sub> heterogeneous and homogeneous oxidation  
 242 to sulfate were 16.5‰ and -9‰, respectively (Tanaka et al., 1994). Consequently, the contribution of  
 243 SO<sub>2</sub> heterogeneous and homogeneous oxidation to sulfate could be calculated by sulfur isotope mass  
 244 equilibrium equations (2) and (3).

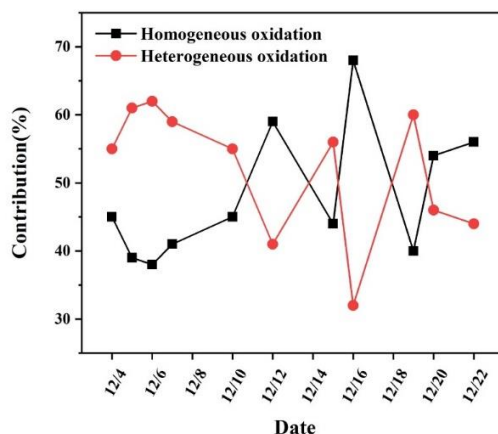
$$245 \quad \delta^{34}\text{S}_{\text{SO}_2} + 16.5x - 9y = \delta^{34}\text{S}_{\text{SO}_4^{2-}} \quad (2)$$

$$246 \quad x + y = 1 \quad (3)$$

247 where x and y represent the contribution of SO<sub>2</sub> heterogeneous and homogeneous oxidation,  
 248 respectively.

249 It is observed from Fig. 6 that most of the days (7 out of 11) had more than 50% contributions from  
 250 SO<sub>2</sub> heterogeneous oxidation, contribution of SO<sub>2</sub> heterogeneous oxidation markedly fluctuated ranging  
 251 from 31.4 to 62.0% with an average and standard deviation at 51.6 ± 0.1%, which indicated that SO<sub>2</sub>  
 252 heterogeneous oxidation was generally dominant during sulfate formation. He et al. (2018) presented  
 253 the observations of oxygen-17 excess of PM<sub>2.5</sub> sulfate collected in Beijing haze from Oct. 2014 to Jan.  
 254 2015, and found the contribution of heterogeneous sulfate production was about 41~54% with a mean  
 255 of 48 ± 5%. The contribution of SO<sub>2</sub> heterogeneous oxidation reached high-level during 5-7 Dec. and on  
 256 19 Dec., which was closely related to the temperature of the atmosphere. The low temperature about  
 257 5°C during these days was favorable for SO<sub>2</sub> dissolution in water and further oxidized to sulfate. On 16  
 258 Dec., the contribution of SO<sub>2</sub> heterogeneous oxidation was at the minimum of 31.4%. The highest  
 259 temperature of 15°C on 16 Dec. restrained SO<sub>2</sub> solubility in aqueous solution and produced lots of

260 gaseous oxidants such as OH radicals to promote SO<sub>2</sub> homogeneous oxidation.



261

262 **Fig. 6.** The contributions of SO<sub>2</sub> heterogeneous and homogeneous oxidation to sulfate.

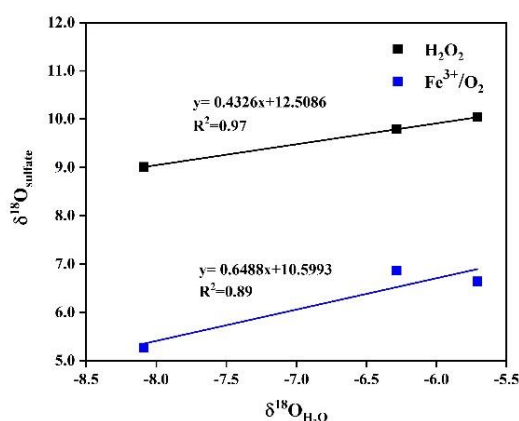
263 Overall, the temperature was an important factor in controlling SO<sub>2</sub> oxidation pathways. High  
264 temperature facilitated kinetic fractionation of sulfur isotope during SO<sub>2</sub> oxidation to sulfate, thereby  
265 decreasing  $\delta^{34}\text{S}$  value in sulfate. In addition, there was lack of positive correlation between the  
266 contribution of SO<sub>2</sub> heterogeneous oxidation and O<sub>3</sub> or NO<sub>2</sub> concentration. This further demonstrated  
267 that SO<sub>2</sub> oxidation by O<sub>3</sub> and NO<sub>2</sub> were not the important pathways during the sampling period.  
268 Consequently, we mainly focused on SO<sub>2</sub> heterogeneous oxidation by H<sub>2</sub>O<sub>2</sub> and Fe<sup>3+</sup>/O<sub>2</sub> in the  
269 following study.

#### 270 3.4 The correlation of $\delta^{18}\text{O}$ values between H<sub>2</sub>O and SO<sub>4</sub><sup>2-</sup> from SO<sub>2</sub> oxidation by H<sub>2</sub>O<sub>2</sub> and Fe<sup>3+</sup>/O<sub>2</sub>

271 It is known that SO<sub>2</sub> rapidly equilibrates with ambient water for very high molar ratio of H<sub>2</sub>O to SO<sub>2</sub>  
272 in the atmosphere. As a result,  $\delta^{18}\text{O}$  value of SO<sub>2</sub> is dynamically controlled by  $\delta^{18}\text{O}$  value of water and  
273  $\delta^{18}\text{O}$  value of SO<sub>2</sub> has no obvious effect on  $\delta^{18}\text{O}$  value of sulfate produced from different oxidation  
274 pathways. Meanwhile, sulfate is very stable with respect to O atom exchange with ambient water.  
275 Consequently,  $\delta^{18}\text{O}$  can be adopted to distinguish SO<sub>2</sub> oxidation processes due to that  $\delta^{18}\text{O}$  value of  
276 product sulfate reflected the distinctive signals of different oxidants.

277 We simulatively studied SO<sub>2</sub> heterogeneous oxidation by H<sub>2</sub>O<sub>2</sub> and Fe<sup>3+</sup>/O<sub>2</sub> in the laboratory, which  
278 aims to make clear the relationship of  $\delta^{18}\text{O}$  values between product sulfate and [three kinds of](#) water at  
279 10 °C. It can be observed from Fig. 7 that  $\delta^{18}\text{O}$  value of sulfate was linearly dependent on  $\delta^{18}\text{O}$  value of  
280 water, and the slope of linear curve for H<sub>2</sub>O<sub>2</sub> oxidation approximates a ratio of 0.43, indicating that the

281 isotopy of about two of four oxygen atoms in sulfate was controlled by  $\delta^{18}\text{O}$  value of water. The other  
 282 two oxygen atoms were from  $\text{H}_2\text{O}_2$  molecules, whose O-O bond remained intact during  $\text{SO}_2$  oxidation.  
 283 In addition, we noted from Fig. 7 that the slope of linear curve for  $\text{Fe}^{3+}/\text{O}_2$  oxidation was about 0.65,  
 284 which represented that the isotopy of about three of four oxygen atoms in sulfate was related to  $\delta^{18}\text{O}$   
 285 value of water. A 3/4 control of sulfate oxygens by water is also characteristic of heterogeneous  
 286 oxidation mechanisms in which  $\text{HSO}_3^-$  isotopically equilibrated with water prior to significant  
 287 oxidation to  $\text{SO}_4^{2-}$ . The other one oxygen atom in sulfate was from  $\text{O}_2$ . The higher slope suggested a  
 288 higher dependence of  $\delta^{18}\text{O}$  value of sulfate on  $\delta^{18}\text{O}$  value of water during  $\text{SO}_2$  heterogeneous oxidation  
 289 by  $\text{Fe}^{3+}/\text{O}_2$ . The discrepancy of the slopes for different  $\text{SO}_2$  heterogeneous oxidation processes provides  
 290 us a potential method to distinguish  $\text{SO}_2$  oxidation pathways.



291  
 292 **Fig.7.** The correlation of  $\delta^{18}\text{O}$  values between  $\text{H}_2\text{O}$  and sulfate from  $\text{SO}_2$  oxidation by  $\text{H}_2\text{O}_2$  and  
 293  $\text{Fe}^{3+}/\text{O}_2$ , respectively.

294 3.5  $\delta^{18}\text{O}\text{-SO}_4^{2-}$  values in  $\text{PM}_{2.5}$  and  $\text{SO}_2$  main oxidation pathways

295 As depicted in Fig. 8,  $\delta^{18}\text{O}$  values of sulfate in  $\text{PM}_{2.5}$  ranged from 11.09 to 12.93‰ with an average  
 296 and standard deviation of  $12.35 \pm 0.68\%$ .  $\delta^{18}\text{O}$  values of sulfate focused on a narrow scope except those  
 297 on 5 and 22 Dec.. It should be pointed out  $\delta^{18}\text{O}$  value of secondary sulfate was a comprehensive result  
 298 from different  $\text{SO}_2$  oxidation processes. Sulfate in  $\text{PM}_{2.5}$  usually consisted of primary sulfate and  
 299 secondary sulfate. The  $\delta^{18}\text{O}$  value of primary sulfate is about 38 ‰ (Holt and Kumar, 1984), which is  
 300 significantly higher than those of secondary sulfate. The contribution of primary and secondary sulfate

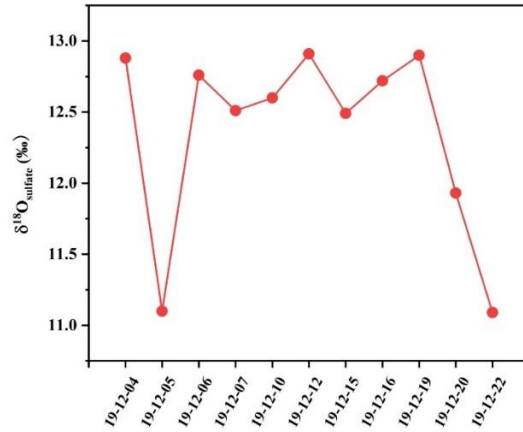


**Fig.8.**  $\delta^{18}\text{O}$  values of sulfate in  $\text{PM}_{2.5}$  during the sampling period.

带格式的: 居中, 缩进: 首行缩进: 0 字符

in the atmosphere can be calculated by oxygen isotope mass equilibrium equation (4) (Ben et al., 1982).

$$\delta^{18}\text{O}_{\text{PM}_{2.5}} = \delta^{18}\text{O}_{\text{PS}} \times (1 - f_{\text{SS}}) + \delta^{18}\text{O}_{\text{SS}} \times f_{\text{SS}} \quad (4)$$

where  $\delta^{18}\text{O}_{\text{PM}_{2.5}}$ ,  $\delta^{18}\text{O}_{\text{PS}}$  and  $\delta^{18}\text{O}_{\text{SS}}$  mean  $\delta^{18}\text{O}$  values of  $\text{PM}_{2.5}$ , primary sulfate and secondary sulfate, respectively;  $f_{\text{SS}}$  is the contribution of secondary sulfate in  $\text{PM}_{2.5}$ .

It is noteworthy from Fig. 9 that there exists a linear relationship between  $\delta^{18}\text{O}$  values in water and secondary sulfate from different  $\text{SO}_2$  oxidation pathways, and this can be described by the equations

(5)-(7), where the value of  $\delta^{18}\text{O}_{\text{water}}$  is about -6.2‰ in Nanjing. As discussed above, secondary sulfate was mainly ascribed to  $\text{SO}_2$  homogeneous oxidation by OH radicals and heterogeneous oxidation by  $\text{H}_2\text{O}_2$  and  $\text{Fe}^{3+}/\text{O}_2$ . Therefore,  $\delta^{18}\text{O}_{\text{SS}}$  value in equation (4) can be obtained based on equations (5)-(7) respectively. As a result, the average contribution of primary and secondary sulfate in  $\text{PM}_{2.5}$  are presented in Table 1. It can be observed that the majority of sulfate in  $\text{PM}_{2.5}$  was secondary sulfate, which appears to constitute from 79.9 to 86.2% of total sulfate during the sampling period. It is admirable to quantitatively describe these formation pathways of secondary sulfate in  $\text{PM}_{2.5}$ .

带格式的: 下标

$$\delta^{18}\text{O}_{\text{sulfate}} = 0.06 \times \delta^{18}\text{O}_{\text{water}} + 3.8 \text{‰ (PS)} \quad (\text{Holt and Kumar, 1984}) \quad (5)$$

$$\delta^{18}\text{O}_{\text{SS}} = 0.69 \times \delta^{18}\text{O}_{\text{water}} + 9.5 \text{‰ (OH)} \quad (\text{Holt and Kumar, 1984}) \quad (5)$$

$$\delta^{18}\text{O}_{\text{SS}} = 0.65 \times \delta^{18}\text{O}_{\text{water}} + 10.6 \text{‰ (Fe}^{3+}/\text{O}_2) \quad (\text{this study}) \quad (6)$$

$$\delta^{18}\text{O}_{\text{SS}} = 0.43 \times \delta^{18}\text{O}_{\text{water}} + 12.5 \text{‰ (H}_2\text{O}_2) \quad (\text{this study}) \quad (7)$$

带格式的: 字体: 10 磅

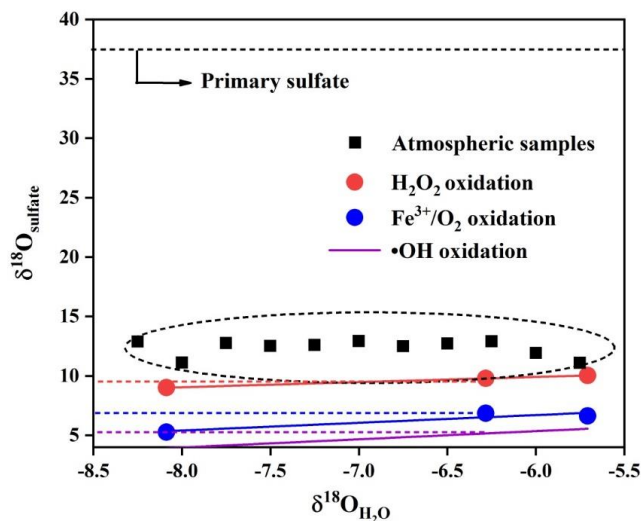


**Fig.9.** The correlation between  $\delta^{18}\text{O}$  values in water and sulfate in  $\text{PM}_{2.5}$ .

**Table 1** The [average](#) contribution of primary sulfate and secondary sulfate in  $\text{PM}_{2.5}$ .

Sampling time	Primary sulfate (%)	Secondary sulfate (%)
4 Dec.	<a href="#">10.9-23.7</a> <a href="#">19.7</a>	<a href="#">76.3-89.1</a> <a href="#">80.3</a>
5 Dec.	<a href="#">4.6-18.2</a> <a href="#">13.9</a>	<a href="#">81.8-95.4</a> <a href="#">86.1</a>
6 Dec.	<a href="#">10.6-23.3</a> <a href="#">19.3</a>	<a href="#">76.7-89.4</a> <a href="#">80.7</a>
7 Dec.	<a href="#">9.6-22.5</a> <a href="#">18.4</a>	<a href="#">77.5-90.4</a> <a href="#">81.6</a>
10 Dec.	<a href="#">10.0-22.8</a> <a href="#">18.7</a>	<a href="#">77.2-90.0</a> <a href="#">81.3</a>
12 Dec.	<a href="#">11.1-23.8</a> <a href="#">20.0</a>	<a href="#">76.2-89.9</a> <a href="#">80.0</a>
15 Dec.	<a href="#">9.6-22.5</a> <a href="#">18.4</a>	<a href="#">77.5-90.4</a> <a href="#">81.6</a>
16 Dec.	<a href="#">11.9-23.6</a> <a href="#">20.1</a>	<a href="#">76.4-88.1</a> <a href="#">79.9</a>
19 Dec.	<a href="#">11.0-23.7</a> <a href="#">19.7</a>	<a href="#">76.3-89.0</a> <a href="#">80.3</a>
20 Dec.	<a href="#">7.7-20.8</a> <a href="#">16.7</a>	<a href="#">79.2-92.3</a> <a href="#">83.3</a>
22 Dec.	<a href="#">4.5-18.1</a> <a href="#">13.8</a>	<a href="#">79.1-95.5</a> <a href="#">86.2</a>

According to the percentages of  $\text{SO}_2$  heterogeneous and homogeneous oxidation to sulfate in Fig.6 and the average contributions of primary sulfate and secondary sulfate in  $\text{PM}_{2.5}$  in Table 1, we can further calculate the ratios of different  $\text{SO}_2$  oxidation pathways at 10 °C via oxygen isotope mass

329 equilibrium equations (8)-(10), and the corresponding results are depicted in Table 2.

$$330 \quad \delta^{18}\text{O}_{\text{PM}_{2.5}} = \delta^{18}\text{O}_{\text{PS}} \times f_{\text{PS}} + (\delta^{18}\text{O}_{\text{SS-OH}} \times f_{\text{SS-OH}} + \delta^{18}\text{O}_{\text{SS-Fe}^{3+}/\text{O}_2} \times f_{\text{SS-Fe}^{3+}/\text{O}_2} + \delta^{18}\text{O}_{\text{SS-H}_2\text{O}_2} \times f_{\text{SS-H}_2\text{O}_2}) \times f_{\text{SS}} \quad (8)$$

$$331 \quad f_{\text{PS}} + f_{\text{SS}} = 1 \quad (9)$$

$$332 \quad f_{\text{SS-OH}} + f_{\text{SS-Fe}^{3+}/\text{O}_2} + f_{\text{SS-H}_2\text{O}_2} = 1 \quad (10)$$

333 where  $\delta^{18}\text{O}_{\text{PM}_{2.5}}$  and  $\delta^{18}\text{O}_{\text{PS}}$  are  $\delta^{18}\text{O}$  values of total sulfate and primary sulfate in  $\text{PM}_{2.5}$ ;  $\delta^{18}\text{O}_{\text{SS-OH}}$ ,  
 334  $\delta^{18}\text{O}_{\text{SS-Fe}^{3+}/\text{O}_2}$  and  $\delta^{18}\text{O}_{\text{SS-H}_2\text{O}_2}$  are  $\delta^{18}\text{O}$  values of secondary sulfate from  $\text{SO}_2$  oxidation by OH radicals,  
 335  $\text{Fe}^{3+}/\text{O}_2$  and  $\text{H}_2\text{O}_2$ , respectively;  $f_{\text{PS}}$  and  $f_{\text{SS}}$  are the contribution of primary and secondary sulfate;  $f_{\text{SS-OH}}$ ,  
 336  $f_{\text{SS-Fe}^{3+}/\text{O}_2}$  and  $f_{\text{SS-H}_2\text{O}_2}$  are the ratios of secondary sulfate from  $\text{SO}_2$  oxidation by OH radicals,  $\text{Fe}^{3+}/\text{O}_2$  and  
 337  $\text{H}_2\text{O}_2$ , respectively.

338 Unlike heavily polluted days with reduced solar irradiation, the photochemical reactivity can remain  
 339 high in clean days during the observation period because of relatively intense solar irradiation. As a  
 340 result, some photochemical reactive species such as OH radicals and  $\text{H}_2\text{O}_2$  are deemed to be the major  
 341 oxidants for sulfate formation. [Generally,  \$\text{H}\_2\text{O}\_2\$  production in the relatively clean atmosphere is](#)  
 342 [ascribed to self-reaction of  \$\text{HO}\_2\$  radicals that mainly come from the reactions of OH radicals with CO](#)  
 343 [and volatile organic compounds.](#) It is observed from Table 2 that the ratios of  $\text{SO}_2$  oxidation by OH  
 344 radicals ranged from 38 to 68% with an average and standard deviation at  $48 \pm 9.7\%$ . The ratio reached  
 345 the maximum of 68% on 16 Dec., which is mainly ascribed to the highest temperature of  $15^\circ\text{C}$  during  
 346 the sampling period. The photochemical reactions are favorable for producing more OH radicals. In  
 347 contrast, the ratio of  $\text{SO}_2$  oxidation by OH radicals decreased to the minimum of 38% on 6 Dec. due to  
 348 the low temperature.

349 **Table 2** The ratios of  $\text{SO}_2$  different oxidation pathways to sulfate.

Time	$f_{\text{SS-OH}}$	$f_{\text{SS-H}_2\text{O}_2}$	$f_{\text{SS-Fe}^{3+}/\text{O}_2}$	$f_{\text{SS-H}_2\text{O}_2} / (f_{\text{SS-H}_2\text{O}_2} + f_{\text{SS-Fe}^{3+}/\text{O}_2})$ (%)
4 Dec.	0.45	0.27	0.28	49.1
5 Dec.	0.39	0.24	0.37	39.3
6 Dec.	0.38	0.24	0.38	38.7
7 Dec.	0.41	0.25	0.34	42.3
10 Dec.	0.45	0.27	0.28	49.1
12 Dec.	0.59	0.30	0.11	73.2
15 Dec.	0.44	0.26	0.30	46.5

带格式的: 非上标/下标

带格式的: 字体: (中文) 宋体, 10 磅

带格式的: 字体: (中文) 宋体, 10 磅

带格式的: 字体: (中文) 宋体, 10 磅

带格式表格



16 Dec.	0.68	0.26	0.06	81.2
19 Dec.	0.40	0.25	0.35	41.6
20 Dec.	0.54	0.31	0.15	67.4
22 Dec.	0.56	0.32	0.12	72.7

350

351 It is known that SO<sub>2</sub> oxidation by H<sub>2</sub>O<sub>2</sub> and Fe<sup>3+</sup>/O<sub>2</sub> are the most important pathways during SO<sub>2</sub>  
352 heterogeneous oxidation. It can be observed from table 2 that the percentage of sulfate from SO<sub>2</sub>  
353 oxidation by H<sub>2</sub>O<sub>2</sub> in secondary sulfate from SO<sub>2</sub> heterogeneous oxidation changed from 38.7 to 81.2%  
354 with an average and standard deviation at 54.6±15.7%, indicating that SO<sub>2</sub> oxidation by H<sub>2</sub>O<sub>2</sub>  
355 predominated during SO<sub>2</sub> heterogeneous oxidation. In addition, there existed an obviously positive  
356 correlation between the ratios of SO<sub>2</sub> oxidation by H<sub>2</sub>O<sub>2</sub> and OH radicals, which was chiefly attributed  
357 to the photochemical reactions. The relatively strong solar irradiation on 16 Dec. resulted in the  
358 maximum ratio of 81.2% about H<sub>2</sub>O<sub>2</sub> oxidation in SO<sub>2</sub> heterogeneous reactions. The sampling site is  
359 close to Nanjing steel plant. As companion emitters, Fe<sup>3+</sup> are present in much higher concentrations  
360 than that in other areas. It is believed that SO<sub>2</sub> oxidation by O<sub>2</sub> in the presence of Fe<sup>3+</sup> was not negligent  
361 in the areas where the concentrations of SO<sub>2</sub> and Fe<sup>3+</sup> were high. This inevitably resulted in high SO<sub>2</sub>  
362 oxidation ratio by Fe<sup>3+</sup>/O<sub>2</sub> in SO<sub>2</sub> heterogeneous oxidation processes.

#### 363 4 Conclusions

364 There was no serious PM<sub>2.5</sub> pollution during the sampling period. The secondary sulfate constitutes  
365 from about 79.9 to 86.2% of total sulfate in PM<sub>2.5</sub>. SO<sub>2</sub> oxidation by O<sub>3</sub> and NO<sub>2</sub> played an  
366 insignificant role in sulfate formation. The secondary sulfate was mainly ascribed to SO<sub>2</sub> homogeneous  
367 oxidation by OH radicals and heterogeneous oxidation by H<sub>2</sub>O<sub>2</sub> and Fe<sup>3+</sup>/O<sub>2</sub>. Compared to  
368 homogeneous oxidation, SO<sub>2</sub> heterogeneous oxidation was generally dominant with an average  
369 contribution of 51.6%. SO<sub>2</sub> oxidation by H<sub>2</sub>O<sub>2</sub> predominated in SO<sub>2</sub> heterogeneous oxidation reactions  
370 and the average ratio of which reached 54.6%. Consequently, sulfur and oxygen isotopes can be used to  
371 gain an insight into sulfate formation. Sulfur isotopic compositions in SO<sub>2</sub> and sulfate were  
372 simultaneously measured to quantify the contributions of SO<sub>2</sub> homogeneous and heterogeneous  
373 oxidation. Combining field observations of oxygen isotope in the atmosphere with the linear  
374 relationships of δ<sup>18</sup>O values between H<sub>2</sub>O and sulfate from different SO<sub>2</sub> oxidation processes can obtain

带格式的: 字体: 10 磅

带格式的: 字体: 10 磅

带格式的: 字体: 10 磅

带格式的: 字体: 10 磅

375 | [an increased understanding of specific sulfate formation pathways. This study is favorable for deeply](#)  
376 | [investigating sulfur cycle in the atmosphere.](#)

377

378 **Author contribution**

379 Ziyang Guo carried out the experiment and wrote the original draft. Keding Lu designed the  
380 methodology and administrated the project. Pengxiang Qiu and Mingyi Xu performed the data  
381 collection. Zhaobing Guo instructed the experiment and revised the paper.

382 **Competing interests**

383 The authors declare that they have no competing interest that can influence the work reported in this  
384 paper.

385 **Acknowledgement**

386 We gratefully acknowledge the financial supports from the National Natural Science Foundation of  
387 China (Nos. 41873016, 51908294, and 21976006), the National Science Fund for Distinguished Young  
388 Scholars (No. 22325601).

389

390

391 **References**

- 392 Abbatt, J. P. D., Benz, S., Cziczo, D. J., Kanji, Z., Lohmann, U., and Mohler, O.: Solid ammonium  
393 sulfate aerosols as ice nuclei: a pathway for cirrus cloud formation, *Science*, 313, 1770-1773,  
394 <https://doi.org/10.1126/science.1129726>, 2006.
- 395 Ben, D. H., Romesh, K., and Paul, T. C.: Primary Sulfates in Atmospheric Sulfates: Estimation by  
396 Oxygen Isotope Ratio Measurements, *Science*, 217, 51-53, <https://doi.org/10.1126/science.217.4554.51>,  
397 1982.
- 398 Brüggemann, M., Riva, M., Perrier, S., Poulain, L., George, C., and Herrmann, H.: Overestimation of  
399 Monoterpene Organosulfate Abundance in Aerosol Particles by Sampling in the Presence of SO<sub>2</sub>,  
400 *Environ. Sci. Technol. Lett.*, 8, 206-211, <https://doi.org/10.1021/acs.estlett.0c00814>, 2021.
- 401 Cheng, Y. F., Zheng, G. J., Wei, C., Mu, Q., Zheng, B., Wang, Z. B., Gao, M., Zhang, Q., He, K. B.,  
402 Carmichael, G., Pöschl, U., and Su, H.: Reactive Nitrogen Chemistry in Aerosol Water as a Source of  
403 Sulfate during Haze Events in China, *Sci. Adv.*, 2, e1601530, <https://doi.org/10.1126/sciadv.1601530>,  
404 2016.
- 405 Gao, J., Wei, Y., Zhao, H., Liang, D., Feng, Y., and Shi, G.: The role of source emissions in sulfate  
406 formation pathways based on chemical thermodynamics and kinetics model, *Sci. Total. Environ.*, 851,  
407 158104, <https://doi.org/10.1016/j.scitotenv.2022.158104>, 2022.
- 408 Guo, Z. B., Shi, L., Chen, S. L., Jiang, W. J., Wei, Y., Rui, M. L., and Zeng, G.: Sulfur isotopic  
409 fractionation and source apportionment of PM<sub>2.5</sub> in Nanjing region around the second session of the  
410 Youth Olympic Games, *Atmos. Res.*, 174-175, 9-17, <https://doi.org/10.1016/j.atmosres.2016.01.011>,  
411 2016.
- 412 Guo, Z. Y., Guo, Q. J., Chen, S. L., Zhu, B., Zhang, Y., Yu, J., and Guo, Z. B.: Study on pollution  
413 behavior and sulfate formation during the typical haze event in Nanjing with water soluble inorganic  
414 ions and sulfur isotopes, *Atmos. Res.*, 217, 198-207, <https://doi.org/10.1016/j.atmosres.2018.11.009>,  
415 2019.
- 416 Han, X. K., Guo, Q. J., Liu, C. Q., Fu, P. Q., Strauss, H., Yang, J., Jian, H., Wei, L., Hong, R., Peters,  
417 M., Wei, R. F., and Tian, L.: Using stable isotopes to trace sources and formation processes of sulfate  
418 aerosols from Beijing, China, *Sci. Rep.*, 6, 29958, <https://doi.org/10.1038/srep29958>, 2016.
- 419 Han, X. K., Guo, Q. J., Strauss, H., Liu, C. Q., Hu, J., Guo, Z. B., Wei, R. F., Peters, M., Tian, L., and

420 Kong, J.: Multiple Sulfur Isotope Constraints on Sources and Formation Processes of Sulfate in Beijing  
421 PM<sub>2.5</sub> Aerosol, Environ. Sci. Technol., 51, 7794-7803, <https://doi.org/10.1021/acs.est.7b00280>, 2017.

422 Harris, E., Sinha, B., Hoppe, P., and Ono, S.: High-precision measurements of <sup>33</sup>S and <sup>34</sup>S fractionation  
423 during SO<sub>2</sub> oxidation reveal causes of seasonality in SO<sub>2</sub> and sulfate isotopic composition, Environ. Sci.  
424 Technol., 47, 12174-12183, <https://doi.org/10.1021/es402824c>, 2013.

425 Harris, E., Sinha, B., Hoppe, P., Crowley, J. N., Ono, S., and Foley, S.: Sulfur isotope fractionation  
426 during oxidation of sulfur dioxide: gas-phase oxidation by OH radicals and aqueous oxidation by H<sub>2</sub>O<sub>2</sub>,  
427 O<sub>3</sub> and iron catalysis, Atmos. Chem. Phys., 12, 407-424, <https://doi.org/10.5194/acp-12-407-2012>,  
428 2012.

429 He, P. Z., Alexander, B., Geng, L., Chi, X. Y., Fan, S. D., Zhan, H. C., Kang, H., Zheng, G. J., Cheng, Y.  
430 F., Su, H., Liu, C., and Xie, Z. Q.: Isotopic constraints on heterogeneous sulfate production in Beijing  
431 haze, Atmos. Chem. Phys., 18, 5515-5528, <https://doi.org/10.5194/acp-18-5515-2018>.

432 He, X., Wu, J. J., Ma, Z. C., Xi, X., and Zhang, Y. H.: NH<sub>3</sub>-promoted heterogeneous reaction of SO<sub>2</sub> to  
433 sulfate on α-Fe<sub>2</sub>O<sub>3</sub> particles with coexistence of NO<sub>2</sub> under different relative humidities, Atmos.  
434 Environ., 262, 118622, <https://doi.org/10.1016/j.atmosenv.2021.118622>, 2021.

435 [Holt, B.D. and Kumar R.: Oxygen-18 study of high-temperature air oxidation of SO<sub>2</sub>. Atmos. Environ.,](#)  
436 [18, 2089-2094, https://doi.org/10.1016/0004-6981\(84\)90194-X, 1984.](#)

437 Huang, R. J., Zhang, Y., Bozzetti, C., Ho, K. F., Cao, J. J., Han, Y., Daellenbach, K. R., Slowik, J. G.,  
438 Platt, S. M., Canonaco, F., Zotter, P., Wolf, R., Pieber, S. M., Bruns, E. A., Crippa, M., Ciarelli, G.,  
439 Piazzalunga, A., Schwikowski, M., Abbaszade, G., Schnelle-Kreis, J., Zimmermann, R., An, Z., Szidat,  
440 S., Baltensperger, U., El Haddad, I., and Prevot, A. S.: High secondary aerosol contribution to  
441 particulate pollution during haze events in China, Nature, 514, 218-222,  
442 <https://doi.org/10.1038/nature13774>, 2014.

443 Kuang, B., Zhang, F., Shen, J., Shen, Y., Qu, F., Jin, L., Tang, Q., Tian, X., and Wang, Z.: Chemical  
444 characterization, formation mechanisms and source apportionment of PM<sub>2.5</sub> in north Zhejiang Province:  
445 The importance of secondary formation and vehicle emission, Sci. Total. Environ., 851, 158206,  
446 <https://doi.org/10.1016/j.scitotenv.2022.158206>, 2022.

447 Li, J. H. Y., Zhang, Y. L., Cao, F., Zhang, W., and Michalski, G.: Stable Sulfur Isotopes Revealed a  
448 Major Role of Transition-Metal Ion-Catalyzed SO<sub>2</sub> Oxidation in Haze Episodes, Environ. Sci. Technol.,

带格式的: 下标

域代码已更改

带格式的: 超链接, 字体: (默认)  
Times New Roman, (中文) 等线, 字  
体颜色: 自动设置

449 54, 2626-2634, <https://doi.org/10.1021/acs.est.9b07150>, 2020.

450 Lin, Y. C., Yu, M., Xie, F., and Zhang, Y.: Anthropogenic Emission Sources of Sulfate Aerosols in  
451 Hangzhou, East China: Insights from Isotope Techniques with Consideration of Fractionation Effects  
452 between Gas-to-Particle Transformations, *Environ. Sci. Technol.*, 56, 3905-3914.  
453 <https://doi.org/10.1021/acs.est.1c05823>, 2022.

454 Liu, M. X., Song, Y., Zhou, T., Xu, Z. Y., Yan, C. Q., Zheng, M., Wu, Z. J., Hu, M., Wu, Y. S., and Zhu,  
455 T.: Fine particle pH during severe haze episodes in northern China, *Geophys. Res. Lett.*, 44, 5213-5221,  
456 <https://doi.org/10.1002/2017GL073210>, 2017.

457 Liu, T., Clegg, S. L., Abbatt, J. P. D.: Fast oxidation of sulfur dioxide by hydrogen peroxide in  
458 deliquesced aerosol particles, *Proc. Natl Acad. Sci. USA.*, 117, 1354-1359,  
459 <https://doi.org/10.1073/pnas.1916401117>, 2020.

460 Liu, Y. Y., Wang, T., Fang, X. Z., Deng, Y., Cheng, H. Y., Nabi, I., and Zhang, L.: Brown carbon: An  
461 underlying driving force for rapid atmospheric sulfate formation and haze event, *Sci. Total. Environ.*,  
462 734, 139415, <https://doi.org/10.1016/j.scitotenv.2020.139415>, 2020.

463 Meng, X., Hang, Y., Lin, X., Li, T. T., Wang, T. J., Cao, J. J., Fu, Q. Y., Dey, S., Huang, K., Liang, F. C.,  
464 Kan, H. D., Shi, X. M., and Liu, Y.: A satellite-driven model to estimate long-term particulate sulfate  
465 levels and attributable mortality burden in China, *Environ. Int.*, 171, 107740,  
466 <https://doi.org/10.1016/j.envint.2023.107740>, 2023.

467 Oh, S. H., Park, K., Park, M., Song, M., Jang, K. S., Schauer, J. J., Bae, G. N., and Bae, M. S.:  
468 Comparison of the sources and oxidative potential of PM<sub>2.5</sub> during winter time in large cities in China  
469 and South Korea, *Sci. Total. Environ.*, 859, 160369, <https://doi.org/10.1016/j.scitotenv.2022.160369>,  
470 2023.

471 Ramanathan, V., Crutzen, P. J., Kiehl, J. T., and Rosenfeld, D.: Aerosols, climate, and the hydrological  
472 cycle, *Science*, 294, 2119-2124, <https://doi.org/10.1126/science.1064034>, 2001.

473 Seinfeld, J. H. and Pandis, S. N.: Atmospheric Chemistry and Physics: From Air Pollution to Climate  
474 Change, *Phys. Today*, 51, 88-90, <https://doi.org/10.1063/1.882420>, 1998.

475 Shao, J., Chen, Q., Wang, Y., Lu, X., He, P., Sun, Y., Shah, V., Martin, R. V., Philip, S., Song, S., Zhao,  
476 Y., Xie, Z., Zhang, L., and Alexander, B.: Heterogeneous sulfate aerosol formation mechanisms during  
477 wintertime Chinese haze events: air quality model assessment using observations of sulfate oxygen

478 isotopes in Beijing, *Atmos. Chem. Phys.*, 19, 6107-6123, <https://doi.org/10.5194/acp-19-6107-2019>,  
479 2019.

480 Tanaka, N., Rye, D. M., Xiao, Y., and Lassaga, A. C.: Use of stable sulfur isotope systematic for  
481 evaluating oxidation reaction pathways and in-cloud scavenging of sulfur dioxide in the atmosphere,  
482 *Geophys. Res. Lett.*, 21, 1519-1522, <https://doi.org/10.1029/94GL00893>, 1994.

483 Wang, G. H., Zhang, R. Y., Gomez, M. E., Yang, L. X., Levy Zamora, M., Hu, M., Lin, Y., Peng, J. F.,  
484 Guo, S., Meng, J. J., Li, J. J., Cheng, C. L., Hu, T. F., Ren, Y. Q., Wang, Y. S., Gao, J., Cao, J. J., An, Z.  
485 S., Zhou, W. J., Li, G. H., Wang, J. Y., Tian, P. F., Marrero-Ortiz, W., Secrest, J., Du, Z. F., Zheng, J.,  
486 Shang, D. J., Zeng, L. M., Shao, M., Wang, W. G., Huang, Y., Wang, Y., Zhu, Y. J., Li, Y. X., Hu, J. X.,  
487 Pan, B., Cai, L., Cheng, Y. T., Ji, Y. M., Zhang, F., Rosenfeld, D., Liss, P. S., Duce, R. A., Kolb, C. E.,  
488 and Molina, M. J.: Persistent sulfate formation from London Fog to Chinese haze, *Proc. Natl. Acad. Sci.*  
489 *U.S. A.*, 113, 13630-13635, <https://doi.org/10.1073/pnas.1616540113>, 2016.

490 Wang, W., Liu, M., Wang, T., Song, Y., and Ge, M.: Sulfate formation is dominated by  
491 manganese-catalyzed oxidation of SO<sub>2</sub> on aerosol surfaces during haze events, *Nature Communications*,  
492 12, 1993, <https://doi.org/10.1038/s41467-021-22091-6>, 2021.

493 Xue, J., Yuan, Z., Griffith, S. M., Yu, X., Lau, A. K. H., and Yu, J. Z.: Sulfate Formation Enhanced by a  
494 Cocktail of High NO<sub>x</sub>, SO<sub>2</sub>, Particulate Matter, and Droplet pH during Haze-Fog Events in Megacities  
495 in China: An Observation-Based Modeling Investigation, *Environ. Sci. Technol.*, 50, 7325-7334,  
496 <https://doi.org/10.1021/acs.est.6b00768>, 2016.

497 Xue, J., Yuan, Z., Yu, J. Z., and Lau, A. K. H.: An Observation-Based Model for Secondary Inorganic  
498 Aerosols, *Aerosol Air Qual. Res.*, 14, 862-878, <https://doi.org/10.4209/aaqr.2013.06.0188>, 2014.

499 Yang, T., Xu, Y., Ye, Q., Ma, Y. J., Wang, Y. C., Yu, J. Z., Duan, Y. S., Li, C. X., Xiao, H. W., Li, Z. Y.,  
500 Zhao, Y., and Xiao, H. Y.: Spatial and diurnal variations of aerosol organosulfates in summertime  
501 Shanghai, China: potential influence of photochemical processes and anthropogenic sulfate pollution,  
502 *Atmos. Chem. Phys.*, 23, 13433-13450, <https://doi.org/10.5194/acp-23-13433-2023>, 2023.

503 Ye, C., Liu, P. F., Ma, Z. B., Xue, C. Y., Zhang, C. L., Zhang, Y. Y., Liu, J. F., Liu, C. T., Sun, X., and  
504 Mu, Y. J.: High H<sub>2</sub>O<sub>2</sub> Concentrations Observed during Haze Periods during the Winter in Beijing:  
505 Importance of H<sub>2</sub>O<sub>2</sub> Oxidation in Sulfate Formation, *Environ. Sci. Technol. Lett.*, 5, 757-763,  
506 <https://doi.org/10.1021/acs.estlett.8b00579>, 2018.

507 Zhang, R., Sun, X. S., Shi, A. J., Huang, Y. H., Yan, J., Nie, T., Yan, X., and Li, X.: Secondary  
508 inorganic aerosols formation during haze episodes at an urban site in Beijing, China, *Atmos. Environ.*,  
509 177, 275-282, <https://doi.org/10.1016/j.jes.2022.01.008>, 2018.

510 Zhang, Y., Bao, F. X., Li, M., Xia, H. L., Huang, D., Chen C. C., and Zhao, J. C.: Photoinduced Uptake  
511 and Oxidation of SO<sub>2</sub> on Beijing Urban PM<sub>2.5</sub>, *Environ. Sci. Technol.*, 54,  
512 14868-14876, <https://doi.org/10.1021/acs.est.0c01532>, 2020.